

Preferential radiation damage of the oxygen sublattice in $\text{YBa}_2\text{Cu}_3\text{O}_7$: A molecular-dynamics simulation

F. Z. Cui

*Chinese Center of Advanced Science and Technology (CCAST) (World Laboratory), P. O. Box 8730, Beijing 100 080, China
and Department of Materials Science and Engineering, Tsinghua University, Beijing 100 084, China*

J. Xie and H. D. Li

*Department of Materials Science and Engineering, Tsinghua University, Beijing 100 084, China
(Received 6 April 1992)*

We study the energetic ionic-displacement processes in orthorhombic $\text{YBa}_2\text{Cu}_3\text{O}_7$ by carrying out a molecular-dynamics simulation based on a pair potential mode. The model crystal contains 3328 atoms. In calculating the time evolution of the partial radial pair-distribution functions during the atomic-collision cascade, we observed preferential radiation damage of the oxygen sublattice in $\text{YBa}_2\text{Cu}_3\text{O}_7$. Detailed features of the preferential radiation damage in the lattice structure were revealed. Oxygen focusing whose displacement threshold may be as low as about 10 eV or less is found to play a dominant role in preferential-radiation-damage processes.

Radiation-damage mechanism in high- T_c superconductors (HTSC), particularly in $\text{YBa}_2\text{Cu}_3\text{O}_7$ (YBCO), have attracted much interest because significant radiation sensitivity in these materials has been found experimentally, such as radiation-induced enhancement of flux pinning and improvement of critical current densities.^{1,2} In addition, knowledge of radiation-damage processes in HTSC is also essential for their applications, for example, in superconducting magnets of fusion reactors and in ion-beam processing of superconducting electronic devices.

Except at very high energy ($> \text{MeV/nucleon}$) of irradiation, nuclear energy loss is known^{3,4} to be the dominant mechanism leading to radiation damage of a YBCO crystal lattice. However, a clear physical picture of the ionic displacement process by elastic collisions between ions in YBCO has not been available to date, although much detailed understanding of radiation-damage processes in metals and normal oxides had already been achieved.^{5,6} Since orthorhombic YBCO is an oxygen-deficient layered perovskite structure with the c axis tripled⁷ and thus with a lower symmetry and with more complexity than that of metals and normal oxides, special mechanisms for radiation-damage processes are expected to be active in these materials. It is generally assumed that radiation-induced displacements in the oxygen sublattice are largely determined by the displacement cross-section mass dependence and the compositional ratio,⁸ although no experimental evidence for this assumption has been given to date. *In situ* standard and high-resolution transmission electron microscopy have been shown some extended defects in ion- and neutron-irradiated samples, but the oxygen atoms remain invisible.^{9,10} Molecular-dynamics (MD) simulation can help elucidate this proposed mechanism of preferential radiation damage in the oxygen sublattice. Very recently, Kirsanov and Musin¹¹ have investigated the radiation-damage process of Cu-O collision

chains along a $\langle 100 \rangle$ direction (c axis) in YBCO by means of MD simulations, and observed two ways of point-defect formation. They used a model crystal of only 189 atoms, in which the containment was inadequate for a proper investigation of radiation-damage dynamics.

In this paper we describe MD simulations of radiation-induced ionic-displacement events in YBCO by using a model crystal of 3328 atoms. The simulated primary knock-on atoms (PKA) can have an initial kinetic energy of up to several hundred eV. By monitoring the evolution of the partial radial pair-distribution function $g(r)$ of four sublattices, the preferential radiation damage of the O sublattice is observed as expected from the theoretical considerations mentioned above. Additional insight into the mechanism was obtained by investigating the effect of the lattice structure in influencing the energy spread of the energetic-ionic-displacement spike in the YBCO crystal. Focusing¹² of oxygen with high efficiency and a low displacement threshold energy (E_d) of oxygen PKA in several low-index crystallographic directions were observed.

The ionic interactions were described by the unscreened rigid-ionic potentials of Chaplot's model,¹³ which reproduced the reasonable crystalline structure and lattice dynamics near the equilibrium state. At short range the pair potential has been modified by an inverse-power potential so as to match a screened Coulomb potential, i.e., the Kr-C universal potential.¹⁴ The whole pair potential function is given as

$$V(r \leq r_1) = V_{\text{Kr-C}},$$

$$V(r_2 < r < r_1) = \lambda_1/(r^n) + \lambda_2/(r^m),$$

$$V(r \geq r_2) = V_{\text{Chaplot}},$$

where parameters of m , n , λ_1 , and λ_2 were determined by

an interpolation scheme in which the value and the first derivative of the matched potentials are guaranteed to be correct at the interpolation points, i.e., r_1 and r_2 . r_1 is taken to be about half of the equilibrium separation (r_{eq}). r_2 is simply taken as r_{eq} for an anion-anion or cation-cation pair and is determined by $V_{Chaplot}(r_2)=1.0$ eV for a cation-anion pair.

The simulations were performed with an orthorhombic crystal model containing $8a \times 8b \times 4c$ unit cells, where \mathbf{a} , \mathbf{b} , and \mathbf{c} are the primitive cell vectors. Notation of Cu(1)-O(1) chain along the b axis in the basal (001) plane is used in this paper. A boundary model of elastic continuum¹⁵ was used, in which the boundary ions were acted by a constant force, a spring force, and a viscous force. In our case the boundary ions are in the first four layers near the boundary of the crystallite. The damping constants of the viscous force have been taken as $M_i \times 10^{14}$ kg/s, where M_i is atomic mass (amu) of the i th ion atom type. Since the initial energy of PKA in the simulations is less than keV, electronic energy loss was not included. We used a crystal model of 0 K temperature. The standard Ewald summation method is incorporated into our program to accelerate the convergence of Coulombic interaction series. The stability of the created damage was tested by a prolonged calculation up to the full step of the crystallite's ions. Checks on energy conservation were used to monitor the time step.

Evidence for the preferential radiation damage of the O sublattice in YBCO is presented in Fig. 1 where the evolution of $g(r)$ for O, Cu, and Ba atoms located within the central 50 cells at two constants, i.e., $t=0.2$ and 0.8 ps are shown, respectively. g_0 denotes the coordination number at equilibrium separation, r_0 , in the simulated crystal at $t=0$. The ionic-displacement event was initiated by Cu(1) PKA of 0.45 keV. The direction of the PKA was chosen at random, i.e., 35° to $\langle 100 \rangle$ and 50° to $\langle 010 \rangle$. Since the results of Y is very similar to that of Ba, they are not shown here. Note that the changes of peak values of $g(r)$ from $t=0$ to $t=0.2$ and 0.8 ps are remarkably different for the three sublattices. At $t=0.2$ ps, six peaks of $g(r)$ for r less than 6 Å in the Ba sublattice, the ratio of the first peak value at $t=0$ and 0.2 ps is 6.67, and the two close peaks (at $r_0=3.82$ and 3.88 Å) became indistinct. In the O sublattice, the first three peaks of $t=0$ had merged into the first peak and the g_0/g at $r=3.21$ Å was 42.1. As the cascade proceeded to 0.8 ps, the $g(r)$ of O atoms showed nearly disordered state, while the peak of $g(r)$ of the Cu and Ba sublattices were further diffused but still persisted to different extents. After $t=0.8$ ps, the shapes of $g(r)$ remained essentially the same till 1.2 ps. These data thus give a quantitative representation for the process of preferential radiation damage of the O sublattice.

representation for the process of preferential radiation damage of the O sublattice.

In order to investigate the detailed mechanism on the preferential radiation damage of the O sublattice, a number of energetic-ionic-displacement events with different initial conditions have been simulated by monitoring the atomic trajectories during the cascade process. Although the detailed trajectories of atoms varied from one event

to another, the general picture reveals some features on the preferential displacement of O atoms in YBCO. Figure 2 shows a random displacement cascade generated by a 200 eV O (1) PKA (denoted as A in the figure) at 59° to $\langle 010 \rangle$ in the basal (001) plane.

A conspicuous feature in the figure is either the strong disturbance of oxygen atoms around their sites or even simple departures from their original sites during the cascade process. This feature has been observed in all cases of ionic-displacement events that we studied. Such an athermal disturbance contributes substantially to the flattening of $g(r)$ of the O sublattice. As shown in Fig. 2, O(1) recoils often fall into O(5) sites at $(0.5a, 0, 0)$, forming Frenkel pair defects. We have verified that for an O(1)-to-O(5) displacement, E_d is 1.5 eV, which is close to

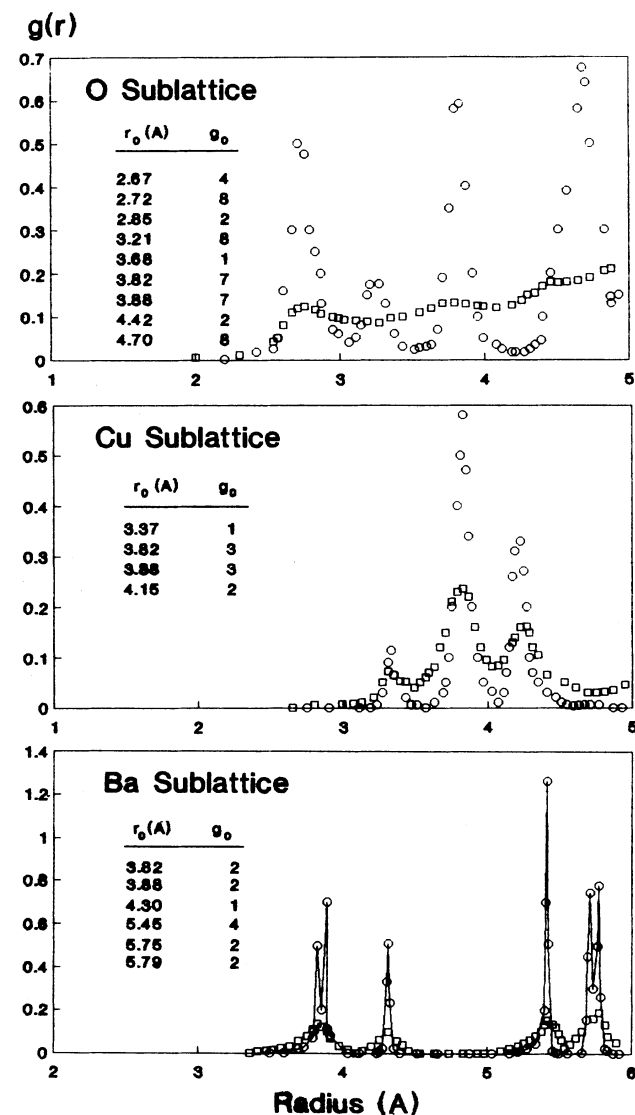


FIG. 1. Partial radial pair-distribution functions $g(r)$ at $t=0.2$ ps (circle point) and $t=0.8$ ps (square point) of a 0.45 keV random cascade of Cu(1) PKA for the oxygen, copper and barium sublattices. g_0 data in the inset are coordination numbers at equilibrium distances r_0 in the simulated YBCO crystal at $t=0$. Curve connecting circle points of Ba is a guide to the eye.

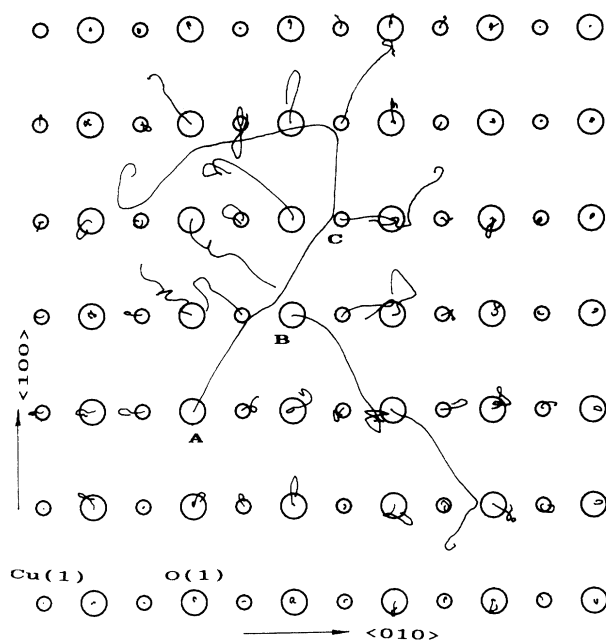


FIG. 2. Atomic trajectories for an ionic-displacement event of 200 eV O(1) PKA at 59° to $\langle 010 \rangle$ in basal (001) plane. More than six O(1) ions fall down to O(5) sites and at least one Cu(1) ion is displaced.

the O-diffusion activation energy of 1.3 eV.¹⁶ Similarly, other Frenkel pairs with short vacancy-interstitial separation in (010) and (100) planes were observed, e.g., O(4) recoil to an O(5) site with $E_d = 4$ eV, O(2), or O(3) recoil to an interstitial site in the middle of two Cu(2) sites [denoted as O(6)] with an E_d less than 9 eV.

Another characteristic feature of the preferential O-sublattice radiation damage of the O sublattice is that O focusing appeared with higher efficiency than Cu focusing or other focusing along anion-cation chains. In Fig. 2, the O(1) focusing along $\langle 110 \rangle$ commences from a random collision cascade. The initial direction of the first O(1) recoil (denoted as B in Fig. 2) in the focusing replacement chain, when it acquired a maximum kinetic energy of 18.9 eV, was at 24.3° to $\langle 110 \rangle$. This indicated that critical angle of formation of O(1) focusing along $\langle 110 \rangle$ is rather high. For O(1) focusing along $\langle 110 \rangle$, the threshold energy of formation of a stable replacement, which is equal to E_d by definition in this case, was determined to be as low as 9 eV. In the (001) basal plane O(1) focusing along $\langle 100 \rangle$ was found to be another replacement-collision sequence that occurs easily for creating a stable Frenkel pair defect. E_d in the vicinity of O(1) focusing along $\langle 100 \rangle$ is only 7 eV in our mode. In order to show the high efficiency in transferring kinetic energy along the two focusing modes, we present Fig. 3 where time dependence of the kinetic energy in the two collision chains caused by a O(1) PKA of 50 eV is given. Note that average energy loss at each step is only 7.5 eV in the O focusing along $\langle 100 \rangle$ and 9 eV in O focusing along $\langle 110 \rangle$. From the data in Fig. 3, we have estimated the velocities of focused-O-atom propagation. Velocities of 4.5×10^6 cm/s for O(1) focusing along $\langle 110 \rangle$ and

3.6×10^6 cm/s for O(1) focusing along $\langle 100 \rangle$ were obtained, which are close to the typical phonon velocity in solids, i.e., 5×10^6 cm/s.¹⁷ This motion may be considered to be a kind of shock wave.

The relatively inefficient focusing process in the focusing chains involving cations is also observed in Fig. 2. The initial direction of motion of the Cu(1) recoil denoted as C in Fig. 2, when it received a maximum kinetic energy of 28.5 eV, was very close to the focusing direction of Cu(1)-O(1) $\langle 010 \rangle$, i.e., 4.1° to $\langle 010 \rangle$. But no replacement occurred.

On the basis of the present simulation study, we believe that the mechanism of preferential radiation damage of the O sublattice does operate during the displacement cascade. Our result on the small E_d of O(1)-O(5) displacement is consistent with the idea suggested by Kirk *et al.*¹⁸ and Summers *et al.*¹⁹ of preferential oxygen redistribution in the a - b plane at the beginning of irradiation experiments, which leads to the orthorhombic to tetragonal transformation. Furthermore, our results show that oxygen redistributions are not limited to within the a - b plane, as the E_d of other displacements, e.g., O(4)-O(5) and O(2)-O(6), are also very low. In addition, the results on the time evolution of $g(r)$ for these four sublattices implies that the primary damage state of the 0.45 keV cascade is a fairly rigid cation sublattice with a background of nearly disordered O ions. This physical picture may be helpful in interpreting the controversial defect structures observed in the irradiated samples by high-resolution electron microscopy, where the images of a vague cation sublattice were still visible in the "distorted regions" of irradiated defects with diameters of about 30 Å or more.¹⁰

The origin of the mechanism of the preferential radiation damage of the O sublattice comes from not only the ionic-displacement cross-section mass dependence and the composition ratio, but also the particular lattice structure. As for the latter, the ejection of focused O ions from the core of the ionic-displacement cascade must play an important role as there is a number of crystallographic directions for the focusing to occur in every unit

Kinetic Energy (eV)

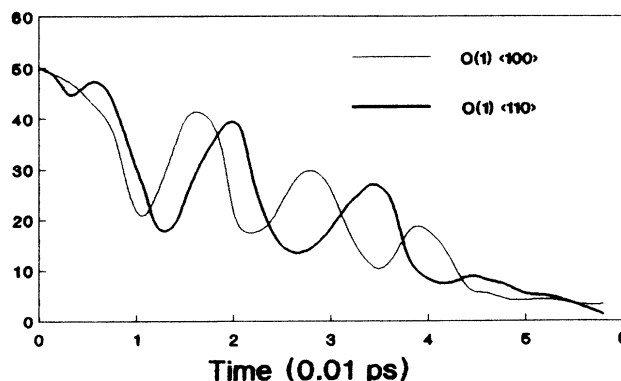


FIG. 3. Kinetic-energy curves for 50 eV O(1) focusing along $\langle 100 \rangle$ (thin line) and along $\langle 110 \rangle$ (thick line). In the $\langle 110 \rangle$ curve, a dip at about 0.4×10^{-14} s is due to a collision with a neighboring Cu(1) ion.

cell of orthorhombic YBCO. As other oxide HTSCs are similar in this respect, the same mechanism of preferential radiation damage of the O sublattice should be operative in all oxide HTSCs.

Along certain directions for O focusing, small E_d (< 10 eV) of O ions was found in the present simulations. These values are much lower than the minimum E_d in metals [> 16 eV (Ref. 20)] and normal oxides [> 40 eV (Ref. 6)]. In almost all the irradiation experiments of HTSC materials—from an early one²¹ to very recent works^{2,3,9}—an average E_d of 20 eV on all sublattices was assumed and used to calculate the basic parameters in question, such as displacements per atom. This value, however, is to be regarded as being open to question in view of our simulation results. At least, the average E_d is not the same for the four sublattices, and of these, the E_d of the O sublattice is the smallest one. For example, the number of displaced atoms caused by the PKA in Fig. 2, taking $E_d = 20$ eV, should be 4 (two Cu ions and two O

ions) according to the modified Kinchin-Pease equation.²² In the simulation, this number is twice the above value and most of this number is of oxygen.

In summary, we report a MD study of the ionic-displacement cascades in YBCO. Our results on the time evolution of $g(r)$ for our sublattices present evidence for a preferential displacement of O ions from its sublattice. The simulations show that O focusing occurs with a much higher efficiency than that along ionic rows involving cations. The E_d of O ions may be as low as several eV.

The computations were performed at the Computer Center of Tsinghua University. It is a pleasure to acknowledge Dr. Ronald Wong and J. Z. Chu for valuable assistance during the course of the work. This work is supported in part by the Chinese Natural Science Foundation.

-
- ¹L. Civale, A. D. Marwick, M. W. McElfresh, T. K. Worthington, A. P. Malozemoff, F. H. Holtzberg, J. R. Thompson, and M. A. Kirk, *Phys. Rev. Lett.* **65**, 1164 (1990).
- ²F. M. Sauerzopf, H. P. Weisinger, W. Kritscha, H. W. Weber, G. W. Crabtree, and J. Z. Liu, *Phys. Rev. B* **43**, 3091 (1991).
- ³B. Hensel, B. Roas, S. Henke, R. Hopfengärtner, M. Lippert, J. P. Ströbel, M. Vildić, G. Saemann-Ischenko, and S. Klaumünzer, *Phys. Rev. B* **42**, 4135 (1990).
- ⁴D. Bourgault, S. Bouffard, M. Toulemonde, D. Groult, J. Provost, F. Studer, N. Nguyen, and B. Raveau, *Phys. Rev. B* **39**, 6549 (1989).
- ⁵T. Diaz de la Rubia and M. W. Guinan, *Phys. Rev. Lett.* **66**, 2766 (1991); T. Diaz de la Rubia, R. S. Averback, R. Renedek, and W. E. King, *Phys. Rev. Lett.* **59**, 1930 (1990).
- ⁶N. Itoh and K. Tanimura, *Radiat. Eff.* **98**, 269 (1986).
- ⁷M. A. Beno, L. Soderholm, D. W. Capone II, D. G. Hinks, J. D. Jorgensen, J. D. Grace, I. K. Schuller, C. U. Segre, and K. Zhang, *Appl. Phys. Lett.* **51**, 57 (1987).
- ⁸See, e.g., M. O. Ruault, H. Bernas, J. Lesueur, L. Dumoulin, M. Nicolas, J. P. Buger, M. Gasgnier, H. Noel, P. Gougeon, N. Potel, and J. C. Levet, *Europhys. Lett.* **5**, 435 (1988); H. Bernas, J. Lesueur, P. Nedellec, M. O. Ruault, L. Dumoulin, and J. P. Burger, *Nucl. Instrum. Methods B* **46**, 269 (1990).
- ⁹M. A. Kirk, M. C. Frischherz, J. Z. Liu, L. R. Greenwood, and H. W. Weber, *Philos. Mag. Lett.* **62**, 41 (1990).
- ¹⁰G. Van Tendeloo, M. O. Ruault, H. Bernas, and M. Gasbnier, *J. Mater. Res.* **6**, 677 (1991).
- ¹¹V. V. Kirsanov and N. N. Musin, *Phys. Lett. A* **153**, 493 (1991).
- ¹²I. M. Torrens and L. T. Chadderton, *Phys. Rev.* **159**, 671 (1967).
- ¹³S. L. Chaplot, *Phys. Rev. B* **42**, 2149 (1990).
- ¹⁴J. Ziegler, J. P. Biersack, and U. Littmark, *The Stopping and Range of Ions in Solids* (Pergamon, New York, 1985), Vol. 1.
- ¹⁵C. Erginsoy, G. H. Vineyard, and A. Englert, *Phys. Rev.* **133**, A595 (1964).
- ¹⁶K. N. Tu, N. C. Neh, S. L. Park, and C. C. Tsuei, *Phys. Rev. B* **39**, 304 (1989).
- ¹⁷C. Kittel, *Introduction of Solid State Physics*, 5th ed. (Wiley, New York, 1976), Chap. 5.
- ¹⁸M. A. Kirk, M. C. Frischherz, J. Z. Liu, L. L. Funk, L. J. Thompson, E. A. Ryan, S. T. Ockers, and H. W. Weber, *Physica C* **162-164**, 532 (1989).
- ¹⁹G. P. Summers, E. A. Burke, D. B. Chrisey, M. Nastasi, and J. R. Tesmer, *Appl. Phys. Lett.* **55**, 1469 (1989).
- ²⁰See, e.g., K. L. Merkle, in *Radiation Damage in Metals*, edited by S. D. Harkness and N. L. Peterson (American Society for Metals, Metals Park, OH, 1976), p. 58.
- ²¹A. E. White, K. T. Short, D. C. Jacobson, J. M. Poate, R. C. Dynes, P. M. Mankiewich, W. J. Skocpol, R. E. Howard, M. Anzlowar, K. W. Baldwin, A. F. J. Levi, J. R. Kwo, T. Hsieh, and M. Hong, *Phys. Rev. B* **37**, 3755 (1988).
- ²²M. T. Robinson and I. M. Torrens, *Phys. Rev. B* **9**, 5008 (1974).